Chemistry & Biology, Vol. 10, 361–368, April, 2003, ©2003 Elsevier Science Ltd. All rights reserved. DOI 10.1016/S1074-5521(03)00075-9

Crystal Structure and Molecular Modeling of 17-DMAG in Complex with Human Hsp90

Joseph M. Jez,[1,4] Julian C.-H. Chen,[2] Giulio Rastelli,[3] Robert M. Stroud,[2] and Daniel V. Santi[1]*
[1]Kosan Biosciences, Inc.
3832 Bay Center Place
Hayward, California 94545
[2]Department of Biochemistry and Biophysics
University of California, San Francisco
San Francisco, California 94143
[3]Dipartimento di Scienze Farmaceutiche
Universita di Modena e Reggio Emilia
Via Campi 183 41100 Modena
Italy

Summary

Hsp90 is an attractive chemotherapeutic target because it chaperones the folding of proteins found in multiple signal transduction pathways. We describe the 1.75 Å resolution crystal structure of human Hsp90α (residues 9–236) complexed with 17-desmethoxy-17-N,N-dimethylaminoethylamino-geldanamycin (17-DMAG). The structure revealed an altered set of interactions between the 17-substituent and the protein compared to geldanamycin and the 17-dimethylaminoethyl moiety pointing into solvent, but otherwise was similar to that reported for the complex with geldanamycin. Targeted molecular dynamics simulations and energetic analysis indicate that geldanamycin undergoes two major conformational changes when it binds Hsp90, with the key step of the conversion being the *trans* to *cis* conformational change of the macrocycle amide bond. We speculate that 17-DMAG analogs constrained to a *cis*-amide in the ground state could provide a significant increase in affinity for Hsp90.

Introduction

Hsp90 is an essential protein that chaperones multiple growth-regulatory signaling proteins, including protein kinases [1] and transcription factors [2, 3]. Geldanamycin (Figure 1A), a benzoquinone ansamycin antibiotic, binds to the N-terminal domain ATP binding site of Hsp90 [4, 5], inhibiting the chaperone activity of the protein. This leads to disruption of the Hsp90 client protein complexes and subsequent ubiquitination and degradation by the proteosome of the client proteins. Because the Hsp90 client proteins are so important in signal transduction and transcription, geldanamycin and its analogs have the potential of serving as chemotherapeutic agents in a number of diseases.

Although geldanamycin displays high potency in cytotoxicity assays, it showed significant hepatotoxicity in preclinical trials [6]. Likely, this can be attributed to the quinone moiety and/or the high reactivity of the 17-C-methoxy group toward nucleophiles. Analogs with 17-alkylamino groups in place of the 17-methoxy moiety have excellent activity in cell-based cytotoxicity assays [7, 8], are less reactive toward nucleophiles, and show reduced hepatotoxicity (vida infra). One of these compounds, 17-allylamino-17-demethoxygeldanamycin (17-AAG; NSC 330507), demonstrated antitumor activity in vivo and was brought into Phase I clinical trials. However, 17-AAG's relative water insolubility makes it difficult to formulate, and early reports indicate some degree of hepatotoxicity that might be averted by more potent analogs. Preclinical evaluation of 17-desmethoxy-17-N,N-dimethylaminoethylamino-geldanamycin (17-DMAG; NSC 707545) showed that it is more potent and water soluble than 17-AAG, is active against in mouse-human xenografts, and has excellent oral bioavailability [9].

Here we report the three-dimensional structure of the N-terminal domain of human Hsp90α complexed with 17-DMAG determined by X-ray crystallography and refined to 1.75 Å resolution. We also report a targeted molecular dynamics study and an energy analysis of the conformational changes that convert the free into the bound conformation of geldanamycin. Taken together, the results presented here provide a structural template for further development of drugs based on the geldanamycin scaffold.

Results and Discussion

Overall Protein Structure

The 1.75 Å resolution crystal structure of 17-DMAG complexed to the N-terminal domain of human Hsp90α was determined using molecular replacement (Table 1). Although the crystallization conditions of the 17-DMAG complex (MPD/pH 4.5) were different from those of the previously published geldanamycin complex (PEG/pH 8.5) [4], crystals of the 17-DMAG complex grew in the same space group ($P2_1$) with unit cell dimensions (a = 47.7 Å; b = 41.7 Å; c = 56.0 Å; β = 102.8°) similar to those of the geldanamycin complex structure (a = 53.7 Å; b = 44.3 Å; c = 54.6 Å; β = 116.1°). The final model comprises residues 9–223, 277 waters, 1 molecule of 17-DMAG, 2 MPD molecules, and 2 acetate molecules. All residues lie within the allowed regions of the Ramachandran plot. There is a single amino acid difference between this structure and the previously published human Hsp90 structure [4]. The 17-DMAG•Hsp90 structure shows a serine at position 63 rather than the threonine reported in the geldanamycin•Hsp90 complex. The presence of Ser63 in our Hsp90 was confirmed by DNA sequencing, and is likewise present in the authentic full-length Hsp90 clone reported by Hickey et al. [10]. We presume that the serine and threonine variants in the structural models reflect the origin of the respective clones.

In the complex with 17-DMAG, the overall structure of the N-terminal domain of human Hsp90α adopts the "open" ATP binding site conformation that allows ligand

*Correspondence: santi@kosan.com
[4]Current address: Danforth Plant Science Center, 975 North Warson Rd., St. Louis, Missouri 63132.

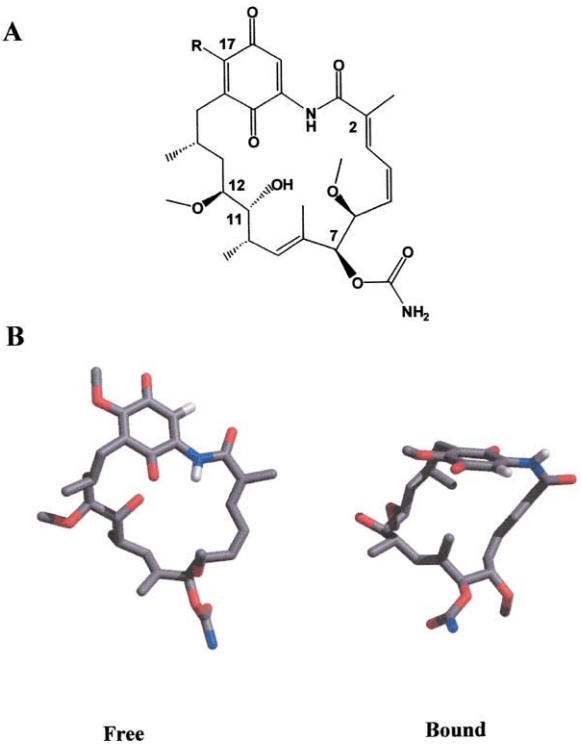

Figure 1. Geldanamycin and Analogs

(A) Structures of geldanamycin (R = CH_3O-) and 17-substituted analogs (17-AAG, R = CH_2=$CHCH_2NH$- and 17-DMAG, R = $(CH_3)_2NCH_2CH_2NH$-).

(B) Conformations of geldanamycin in the free (left) and the Hsp90-bound (right) forms.

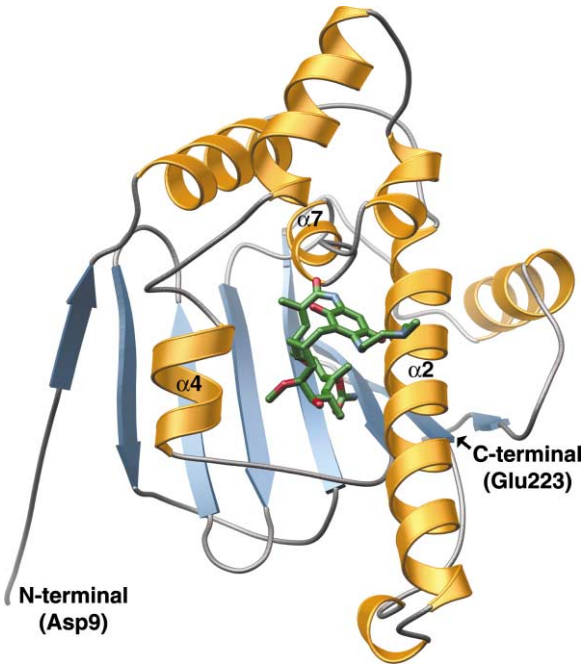

Figure 2. Structure of the Hsp90•17-DMAG Complex

Ribbon representation of the N-terminal domain of human Hsp90α (α helices, gold; β strands, blue) showing the location of 17-DMAG (green ball-and-stick model). The N and C termini residues are indicated.

binding [4] (Figure 2). The 17-DMAG complex structure is similar to the geldanamycin complex structure [4] with a root-mean square deviation (RMSD) of the C_α-atoms of 0.77 Å. The largest local coordinate shifts of 2–4 Å between the protein backbones of the two structures occur between residues 34–37, 115–128, and 156–157. Different loop conformations account for changes in the positions of residues 34–37 and 156–157. With residues 115–128, the changes result from different crystal contacts between the two structures.

17-DMAG Binding in the Active Site

Clear electron density in the ATP binding cleft of Hsp90 indicated unambiguously the location and orientation of 17-DMAG (Figure 3A). The site where 17-DMAG binds is centered between three α helices (α2, α4, and α7) on the face of the core antiparallel β sheet structure (Figure 2). As expected, the interactions between the residues of the binding site and the ansa ring of 17-DMAG are similar to those observed with geldanamycin [4]. Likewise, the network of water molecules observed at the bottom of the binding site in the geldanamycin complex is conserved in the 17-DMAG structure.

Embedded in the ATP/geldanamycin site, the ansa ring of 17-DMAG adopts a C-like conformation with the

Table 1. Data Collection and Refinement Statistics

Space group	$P2_1$
Cell dimensions	*a* = 47.7 Å; *b* = 41.7 Å; *c* = 56.0 Å; β = 102.8°
Resolution	10–1.75 Å
Reflections (total/unique)	97,350/21,560
Completeness (highest shell)	99.2% (97.9%)
$\langle I/\sigma \rangle$ (highest shell)	5.3 (2.2)
R_{sym}[a] (highest shell)	6.5% (31.7%)
R_{cryst}[b]/ R_{free}[c]	18.4%/21.9%
Rms. deviation bond lengths	0.005 Å
Rms. deviation bond angles	1.3°
Average B factor, main chain/side chain	14.9 Å²/18.8 Å²
Average B factor, water	32.4 Å²
Average B factor, 17-DMAG/MPD/acetate	13.5 Å²/46.1 Å²/53.9 Å²

[a] $R_{sym} = \Sigma|I_h - \langle I_h \rangle|/\Sigma I_h$, where $\langle I_h \rangle$ is the average intensity over symmetry equivalent reflections.

[b] $R_{cryst} = \Sigma||F_o| - |F_c||/\Sigma|F_o|$, where summation is over the data used for refinement.

[c] R_{free} is defined the same as R_{cryst} but was calculated using 5% of data excluded from refinement.

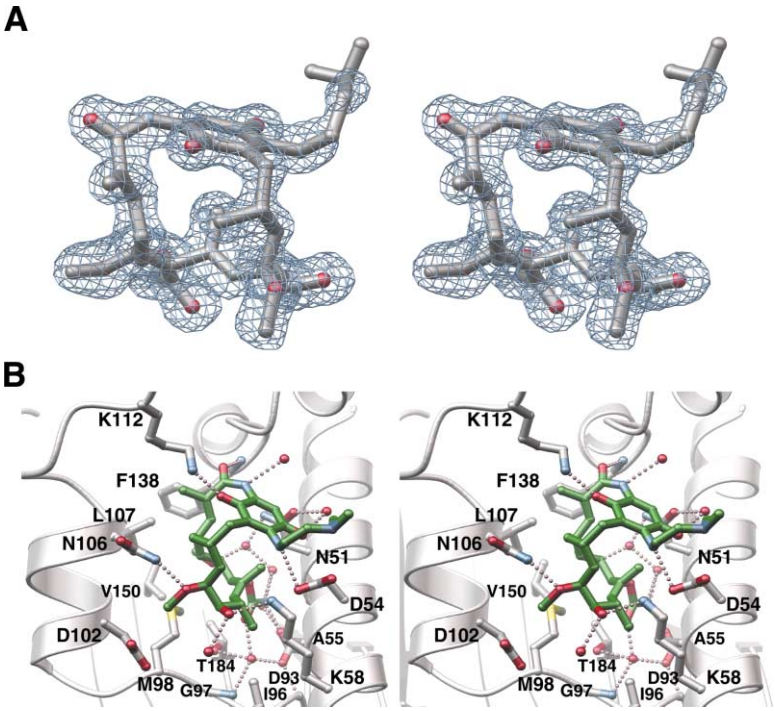

Figure 3. Binding of 17-DMAG

(A) Stereoview of the composite omit, cross-validated, sigma-A weighted map electron density (contoured at 1.2 σ) of 17-DMAG.
(B) Stereoview of residues in the binding cleft. 17-DMAG (green) and waters (red spheres) are also shown. Hydrogen bond interactions are indicated by dotted lines (rose).

carbamate group at the bottom back of the site and the benzoquinone ring at the solvent-exposed top of the pocket (Figure 3B). Multiple protein-ligand interactions (Figure 4) lock the macrocyle of 17-DMAG in a conformation similar to that of geldanamycin. The C7-carbamate group and a water molecule form a hydrogen bond network with the side chains of Asp93 and Thr184 and the backbone nitrogens of Gly95 and Gly97. Extensive van der Waals contacts between the ansa ring of 17-DMAG and binding pocket residues are supplemented by additional hydrogen bonds with other substituents of the macrocycle. The amide of the ansa ring interacts with the backbone nitrogen of Phe138 and a water molecule on the surface of the binding site. The methoxy groups at positions 6 and 12 form hydrogen bonds with the amide nitrogen of Asn106 and a water molecule buried at the back of the site, respectively. Likewise, the amine of Lys58 interacts with the C11-hydroxyl group. Finally, the C18-ketone hydrogen bonds with the amine of Lys112 and the C21-ketone contacts a water molecule that in turn interacts with the amide oxygen of Asn51.

Positioned at the top of the ATP/geldanamycin binding site, the 17-dimethylaminoethylamino substituent of 17-DMAG points into solvent. The electron density is weaker for the dimethylaminoethyl group (Figure 3A) and the B-factors are higher for the atoms of this side chain (average of 30.3 Å^2) compared to those of the ansa ring (average of 10.8 Å^2) also reflecting this moiety's

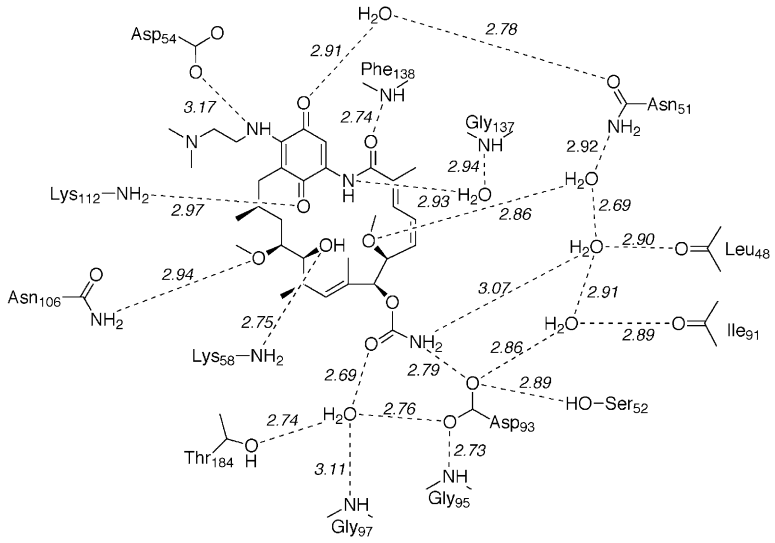

Figure 4. Interactions between 17-DMAG and Hsp90

Schematic drawing of interactions between 17-DMAG and the ATP binding site of human Hsp90α. Hydrogen bonds are shown as dotted lines with distances given in angstroms.

flexibility and its solvent exposure. Although the 17-position side chain of 17-DMAG is longer than the C17-methoxy group of geldanamycin, the dimethylaminoethylamino moiety is oriented into solvent and does not interfere with binding of the ligand to the target site. This observation corroborates structure-activity relationship studies demonstrating that small alkylamino groups, either unfunctionalized or bearing hydroxyl or amino moieties, are the best inhibitors in cell-based toxicity assays [7, 8].

There is a rearrangement of protein-ligand interactions in the binding site accompanying the substitution of an alkylamino group at the 17-position of 17-DMAG for the methoxy moiety of geldanamycin. In the geldanamycin complex, the side chain amine of Lys58 forms hydrogen bonds with both the C11-hydroxyl group and the C17-methoxy group of the macrocycle. With 17-DMAG, the amine of Lys58 only hydrogen bonds with the C11-hydroxyl group, as described above, and a hydrogen bond between the 17-NH group of the substituent and the carboxylate of Asp54 replaces the interaction between the oxygen of the C17-methoxy group of geldanamycin and Lys58. With the altered interactions in the binding site, the position of the quinone ring shifts 0.5–0.8 Å away from Lys58 and toward Asp54. The hydrogen bond between the 17-amino group of 17-DMAG and Asp54 is the only protein-ligand interaction provided by the dimethylaminoethylamino group, since the remainder of the side chain is oriented away from the binding site and into solvent. Based on the 17-DMAG structure, we propose that the 17-alkylamino analogs, including 17-AAG, bind with the 17-NH group, forming a hydrogen bond with Asp54, with the remainder of the side chain pointing into solvent.

Conformational Changes of Geldanamycin from the Free to Bound Forms

As described above, the structure of the Hsp90-bound macrocycle of 17-DMAG closely resembles that reported for bound geldanamycin. It adopts a C-like conformation quite different than the structures of free geldanamycin [11] or 17-azetidinyl-geldanamycin [12]. In the bound conformation, the benzoquinone ring folds over the macrocycle into a highly compact structure with a remarkable rearrangement of the polyketide backbone. Moreover, although obvious from the crystal structures but to our knowledge not explicitly mentioned in previous reports [4, 5], the *trans*-amide bond of the free polyketide is bound to the protein as a *cis*-amide bond (Figure 1B).

To gain insight into the conformational path taken to convert free geldanamycin into the Hsp90-bound form, targeted molecular dynamics (TMD) simulations were employed. Although the time scale of transition in TMD is arbitrary, the relative order of events in the conformational changes is determined by the intrinsic energy surface of the system, and TMD has been highly successful in modeling conformational changes [13-15]. Figure 5 shows superimpositions of averaged structures collected during the time course of an 800 ps TMD simulation, with the stationary points identified along the conversion explicitly shown.

Starting from the free conformation, the 0–360 ps time interval is characterized by the folding of the benzoquinone over the macrocycle. This folding is accompanied by conformational changes at the C10–C15 and the C2–C6 regions of the polyketide. The conformation generated (Intermediate 1 in Figure 5), which lasts between 330 ps and 500 ps, is still significantly open and the amide bond is still *trans*. Remarkably, it is not possible to dock this conformation into Hsp90 without severe steric conflicts with active site residues. Conversion of the amide bond to the *cis* form occurs at about 550 ps. The 360–640 ps frame shows that when the amide bond isomerizes to *cis*, the C11–C15 portion of geldanamycin moves toward the diene moiety, leading to a highly packed C-like structure with the C14-methyl and C2-methyl groups bridging the two halves of the ansa ring (Intermediate 2 in Figure 5). The last conformational change seen at 670 ps involves an axial/equatorial swap of the C11-hydroxyl and the C12-methoxyl groups. This rearrangement moves the C11-hydroxyl group closer to the 17-methoxyl group as seen in the 640–800 ps frame. In the crystal structure of the Hsp90•geldanamycin complex, Lys58 bridges these two groups.

Results from the energetic analysis of geldanamycin in the free, bound, and the two intermediate conformations found by TMD are shown in Table 2 for the MM-PBSA and the molecular orbital AM1 methods. They both predict that the conformation that binds Hsp90 is less stable than the free conformation: the MM-PBSA method by 2.2 kcal mol^{-1} and the AM1 method by 6.4 kcal mol^{-1} (free energy differences in water relative to the free conformation, ΔG_{water}). Intermediates 1 and 2 are 0.4 kcal mol^{-1} and 4.6 kcal mol^{-1} (MM-PBSA) and 1.2 kcal mol^{-1} and 4.5 kcal mol^{-1} (AM1) less stable than the free conformation, respectively. Both methods suggest that the stability of the bound conformation is favored by a higher solvation free energy compared to the free conformation. However, they indicate that there is a significant entropic penalty in the bound conformation. Indeed, while the free and Intermediate 1 conformations are significantly open and coherently have larger entropy values (the ΔS is even positive for Intermediate 1), Intermediate 2 and the bound conformations are highly packed and have lower entropy values. The decrease in entropy when going from the free to the bound form is -3.4 cal mol^{-1} K^{-1} (MM-PBSA) and -5.46 cal mol^{-1} K^{-1} (AM1).

Implications for Inhibitor Design

Several results obtained in this study may be of relevance in future design of inhibitors of the ATPase site of human Hsp90. First, the structures of the ansa ring of 17-DMAG and geldanamycin are nearly identical when bound to Hsp90. Thus, one can be secure in using either structure for conventional structure-based design approaches toward enhancement of 17-methoxy or 17-alkylamino analogs. Second, the alkyl moiety of 17-alkylamino-geldanamycins points toward solvent and appears to be flexible. The speculation that a wide variety of 17-alkyl substitutions should be tolerated by Hsp90 without impact is borne out by structure activity relationship studies at this position [7, 8]. Finally, modeling studies

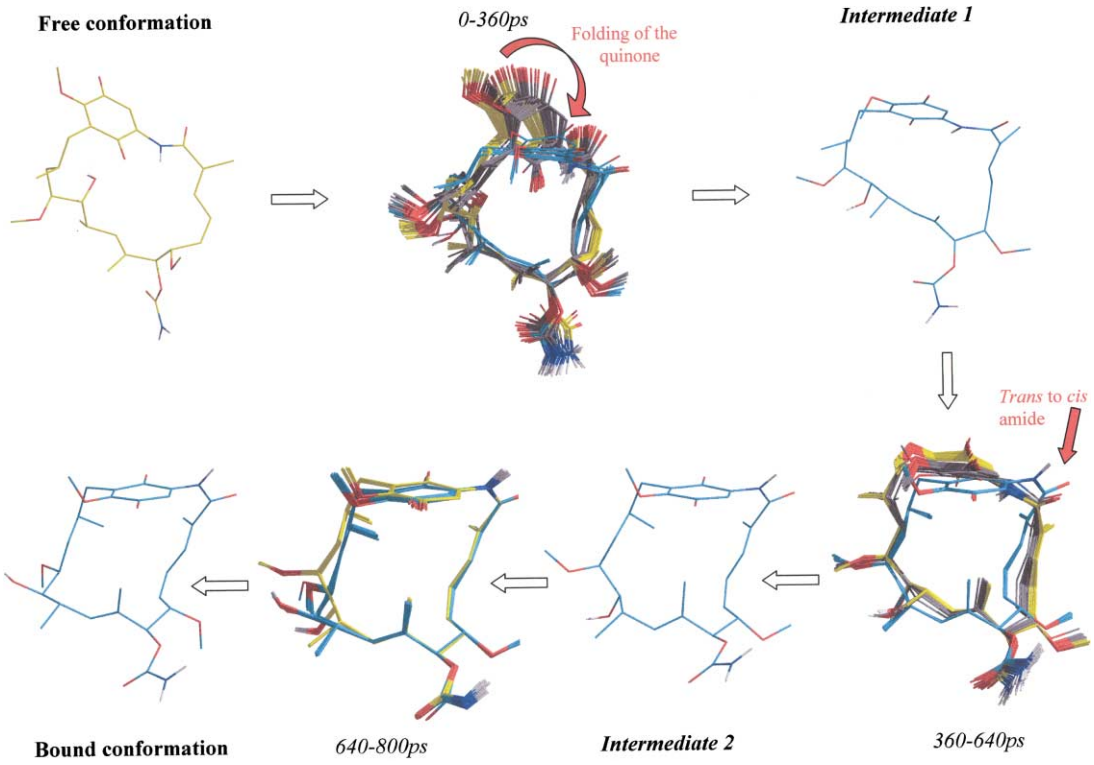

Figure 5. Molecular Dynamics of the Conformational Change of Geldanamycin

Superimposition of averaged structures collected during the 800 ps TMD simulation that converts the free into the bound form of geldanamycin. In the superimpositions, the initial structures are colored in yellow, and the final structures are colored in cyan. The intermediate conformations are explicitly shown. For clarity, only the polar hydrogens are shown.

suggest that geldanamycin undergoes two major conformational changes during the free to bound conversion. The folding of the benzoquinone ring precedes the amide bond conversion, and two intermediate conformations could be detected. Notably, the folding of the quinone by itself is not sufficient to generate a conformation likely to bind Hsp90, while the *trans*-to-*cis* conversion appears to be the more relevant step. Experimental evidence for a large conformational change induced upon binding comes from isothermal titration calorimetry experiments, which show that binding of geldanamycin to Hsp90 suffers a high entropic penalty, while binding of radicicol (which binds without conformational changes) has a favorable entropic contribution [5]. The ΔS values of -3.4 cal mol^{-1} K^{-1} (MM-PBSA) and -5.46 cal mol^{-1} K^{-1} (AM1) calculated here compare well with

Table 2. Energetic Analysis of the Free, Bound, and Intermediate Conformations of Geldanamycin Found by TMD

	H[a]	S[b]	G_{vacuo}[c]	ΔG_{solv}[d]	G_{water}[e]	ΔH[f]	ΔS[f]	ΔG_{vacuo}[f]	ΔG_{water}[f]
MM-PBSA									
Free	52.8 ± 4.8[g]	249.4 ± 1.4	−21.6 ± 4.8	−43.8 ± 1.8	−65.4 ± 4.8	0	0	0	0
Intermediate 1	57.3 ± 4.8	251.5 ± 1.3	−17.7 ± 4.9	−47.3 ± 1.5	−65.0 ± 4.9	4.5	2.1	3.9	0.4
Intermediate 2	61.6 ± 4.9	246.7 ± 0.9	−11.9 ± 4.9	−48.9 ± 1.6	−60.8 ± 4.8	8.8	−2.7	9.7	4.6
Bound	57.5 ± 5.4	246.0 ± 1.7	−15.8 ± 5.4	−47.4 ± 1.6	−63.2 ± 5.4	4.7	−3.4	5.8	2.2
AM1									
Free	−173893.6	268.75	−173973.7	−17.3	−173991.0	0	0	0	0
Intermediate 1	−173892.0	269.19	−173972.3	−17.5	−173989.8	1.6	0.44	1.4	1.2
Intermediate 2	−173887.7	264.05	−173966.4	−20.1	−173986.5	5.9	−4.70	7.3	4.5
Bound	−173887.1	263.29	−173965.6	−19.0	−173984.6	6.5	−5.46	8.1	6.4

[a] Enthalpy (kcal mol^{-1}) at 298.15 K.
[b] Entropy (cal mol^{-1} K^{-1}) at 298.15 K.
[c] Free energy (kcal mol^{-1}) according to $G = H - TS$
[d] Free energy of solvation (kcal mol^{-1})
[e] Free energy in water (kcal mol^{-1}) calculated as $G_{vacuo} + \Delta G_{solv}$
[f] Energy and entropy differences relative to the most stable conformer (kcal mol^{-1})
[g] Averaged values and standard deviations of the 400 ps trajectory.

the measured value of -6.4 cal mol^{-1} K^{-1} (-26.8 J mol^{-1} K^{-1} [5]). We speculate that if a geldanamycin analog had a constrained *cis*-amide bond in the ground state, the remainder of the molecule would adopt the C-like conformation and bind to the open form of Hsp90 without the large energy loss required for a conformational change induced by the protein. If all the energy were conserved by a conformationally restricted analog, one might expect increases in affinity of >1,000-fold. Studies to construct such conformationally constrained analogs are in progress.

Significance

Hsp90 is an essential protein that chaperones the folding of multiple growth-regulatory signaling proteins. In general, disruption of the Hsp90-client protein complexes leads to ubiquitinylation of the client proteins and subsequent degradation by the proteosome. Because the client proteins are so important in signal transduction and transcription, geldanamycin and its analogs have the potential of serving as chemotherapeutic agents in a number of diseases. Use of geldanamycin and 17-allylamino-17-demethoxygeldanamycin (17-AAG) as Hsp90 inhibitors has encountered various problems, including hepatotoxicity and formulation difficulties, thus requiring continued development of new compounds. Preclinical evaluation of 17-desmethoxy-17-N,N-dimethylaminoethylamino-geldanamycin (17-DMAG) shows that it is active against breast cancer, lung cancer, and melanoma xenografts; orally active; and has excellent bioavailability. Determination of the crystal structure of the N-terminal domain of human Hsp90α complexed with 17-DMAG reveals the detailed interactions of this compound with the ATP binding site. Furthermore, targeted molecular dynamics simulations of the conformational changes that convert the macrocyclic ring from the free into the bound conformation suggest that a geldanamycin analog with a constrained *cis*-amide bond in the ground state would bind without the large energy and entropy loss required for the conformational change induced by the protein, resulting in a significant increase in affinity. Taken together, these results provide a structural template for the development of such conformationally constrained Hsp90 inhibitors.

Experimental Procedures

Materials

The pET-28a expression vector was from Novagen. The Ni^{2+}-nitrilotriacetic acid (NTA) agarose was purchased from Qiagen. Benzamidine-Sepharose and the HiLoad 16/60 Superdex-75 FPLC column were from Amersham Biosciences. Thrombin, kanamycin, and isopropyl-1-thio-β-D-galactopyranoside (IPTG) were obtained from Sigma. Amicon centrifugal filter units were purchased from Millipore.

Cloning, Expression, and Purification

The 0.7 kb DNA fragment corresponding to the N-terminal fragment of human Hsp90α [10] (residues 9–236) was excised from pKOS200-236 (A. Schirmer, unpublished data) by restriction digest with NdeI and XhoI and sub-cloned into pET-28a at the same sites. The resulting construct (pKOS227-126) adds an N-terminal hexahistidine tag, a thrombin cleavage site, and a methionine residue before residue 9 of human hsp90α. Transformed *E. coli* BL21(DE3) were grown at 37°C in 1 l of LB media containing 50 μg mL^{-1} kanamycin until A_{600nm} = 0.8–1.0. After induction with 1 mM IPTG, cultures were grown at 30°C for 4–6 hr. Cells were pelleted by centrifugation (10,000 g; 10 min.) and resuspended in 50 ml lysis buffer (50 mM Tris-HCl [pH 8.0], 500 mM NaCl, 20 mM imidazole [pH 8.0], 10% [v/v] glycerol, and 1% [v/v] Tween-20). Following sonication, cell debris was removed by centrifugation (50,000 g; 1 hr) and the supernatant (~500 mg protein) loaded by gravity on a 3 ml Ni^{2+}-NTA agarose column. After washing with 10 column volumes of lysis buffer and 10 column volumes of wash buffer (lysis buffer minus Tween-20), the bound protein was eluted in 50 mM Tris-HCl (pH 8.0), 500 mM NaCl, 250 mM imidazole (pH 8.0), and 10% (v/v) glycerol. Thrombin (~20 μg; weight equal to 1/2000 of eluted protein) was added to the His_6-tagged protein (~40 mg) and dialyzed overnight at 4°C against wash buffer. Dialyzed protein was passed over a 1 ml Ni^{2+}-NTA/benzamidine-Sepharose column (1:1 v/v) equilibrated with 20 column volumes of wash buffer. Gel filtration on a Superdex-75 FPLC column equilibrated with 25 mM Hepes (pH 7.5) and 100 mM NaCl using isocratic conditions for 1.5 column volumes (4 ml fraction size) was the final purification step. The peak fractions (12 mL) were pooled with typical final yields of 30–35 mg of homogenous protein, as determined by SDS-PAGE. Protein was then concentrated using Amicon centrifugal filter units to 35 mg mL^{-1} and stored at −80°C.

Crystallography

For cocrystallization with 17-DMAG, 250 μl of purified protein (0.341 μmol) was mixed with 2 ml of 2.1 mM 17-DMAG (6-fold molar excess) in 25 mM Hepes (pH 7.5) and 100 mM NaCl, then concentrated to 24 mg mL^{-1}. Crystals grew in 3–5 days at 5°C from 2 μl hanging drops of a 1:1 mixture of complexed protein and mother liquor (5%–10% [v/v] 2, 4-methylpentane diol [MPD], 20 mM $CaCl_2$, and 100 mM sodium acetate [pH 4.5]) using the vapor diffusion method. Crystals were dark red/purple in color, suggesting that 17-DMAG was bound in the active site. Prior to freezing in liquid nitrogen, crystals were briefly washed with 35% MPD, 20 mM $CaCl_2$, and 100 mM sodium acetate (pH 4.5). Diffraction data were collected at 105 K from a single crystal on beamline 7-1 of the Stanford Synchrotron Radiation Laboratory (λ = 1.08 Å) using a MAR345 image plate (Table 1). Data were indexed and scaled using MOSFLM [16] and SCALA [17]. The structure was solved by molecular replacement with CNS [18] using the open active site form apoenzyme model of the N-terminal fragment of human Hsp90α (Ref. 4; PDB1YES). Crossrotation and translation searches yielded a single solution (θ_1 = 268.95°, θ_2 = 30.08°, θ_3 = 82.65°, x = 2.56, y = 10.53, z = 27.35) with monitor and packing values of 0.620 and 0.649, respectively, consistent with the presence of a single monomer in the asymmetric unit. After rigid-body refinement using CNS (R_{cryst}=42.4%; R_{free}=42.6%), difference electron density indicated the presence of 17-DMAG in the binding site. Following an initial round of simulated annealing, positional and B-factor refinement (R_{cryst}=30.0%; R_{free}=32.3%,), 17-DMAG was added to the model. CNS parameter and topology files for 17-DMAG were generated using the HIC-Up Server (http://xray.bmc.uu.se/hicup/menu.html). In subsequent iterative rounds of manual rebuilding in O [19] and refinement in CNS, waters were gradually added using CNS with the R-factors converging to those reported in Table 1. All figures were generated using MOLSCRIPT [20] or BOBSCRIPT (http://www.strubi.ox.ac.uk/bobscript) and were rendered with POV-Ray (http://www.povray.org). The coordinates and structure factors for the structure reported in this paper have been deposited in the Protein Data Bank (PDB1OSF).

Molecular Modeling

Molecular dynamics (MD) simulations were performed with the sander module of AMBER7 [21], using the Cornell et al. force field [22] on an IBM-SP3 computer at the Centro Interdipartimentale di Calcolo Elettronico of the University of Modena. Silicon Graphics O2 workstations running MIDAS [23] were used for graphical display. The atomic charges of geldanamycin were obtained from an electrostatic potential (ESP) fit to the 6-31G* ab initio wave function, using GAUSSIAN98, followed by standard RESP [24] fit. Force-field parameters consistent with the Cornell et al. parameterization were assigned and, in a few cases, derived from conformational analysis

performed with AM1. To assure that the resulting conformations were in agreement with the crystal structures, the free and bound forms of geldanamycin were energy minimized. The standard generalized Born/surface area (GB/SA) [25, 26] implicit model for aqueous solvation, with the solvent dielectric set to 80, was used for all simulations. The free conformation of geldanamycin was first minimized with 3,000 steps of conjugate-gradient energy minimization, followed by 200 ps of MD equilibration at 300 K. SHAKE [27] was not used, and a time step of 1 fs was adopted. After equilibration, targeted molecular dynamics (TMD) [28] was used to convert the free (initial structure) into the bound (reference structure) conformation. In TMD, the standard molecular mechanics force-field is supplemented by an additional term based on the mass-weighted root-mean-square deviation (RMSD) of a set of atoms compared to a reference structure. The conformational transition was performed with an 800 ps TMD simulation employing a 1 kcal mol^{-1} force constant to achieve conversion. A longer simulation did not give qualitatively different results. The RMSD of the initial structure was decreased gradually during the simulation, using the weight change option of sander. Coordinates were collected every 0.1 ps and averaged every 10 ps for visual inspection. The energy analysis of geldanamycin in the free, bound, and the two intermediate conformations found by TMD was performed using either the MM-PBSA approach [29] or the AM1 Hamiltonian in the AMSOL [30] package. For MM-PBSA, the free, bound, and intermediate conformations were heated to 300 K in 100 ps and equilibrated for 400 ps without constraints and using the conditions described above, with coordinates collected every 0.1 ps. The averaged structures were in all similar to the structures found by TMD, suggesting that the free, bound, and intermediate conformations seen during the conformational path correspond to true stationary points. The gas-phase energies were calculated for each 0.1 ps snapshot using the same molecular mechanics potential that was used to perform the simulation. The polar contribution to the solvation free energy was calculated using DELPHI [31] with the grid spacing set to 0.5 Å and the dielectric constants inside and outside the molecule set to 1.0 and 80.0, respectively. The nonpolar contribution to the solvation free energy was calculated with the Molsurf [32] program as implemented in AMBER7, using values of γ and b of 0.00542 kcal mol^{-1} $Å^2$ and 0.92 kcal mol^{-1}, respectively, and a probe radius of 1.4 Å. The entropy of geldanamycin was calculated using normal mode analysis. To this end, each snapshot was minimized with a distance-dependent dielectric constant ($\epsilon = 4r$) to include solvent screening effect, until the root-mean-square of the gradient vector was less than $1.0 \cdot 10^{-5}$ kcal mol^{-1} $Å^{-1}$. Then, entropy was estimated with the *nmode* module of AMBER7.

The energetic analysis with the molecular orbital method AM1 in AMSOL [30] was performed with complete geometry optimization and increased convergence criteria. Force constants and vibrational frequencies were calculated on the optimized geometries, and the thermodynamic quantities internal energy, enthalpy, entropy, and free energy were calculated for translation, rotation, and vibrational degrees of freedom at 298.15 K. Enthalpy was determined as the sum of the internal energy plus the zero-point energy correction and the enthalpy required to reach 298.15 K. Free energy G was determined as H-TS, with T = 298.15 K. The solvation free energy was determined using the SM2 [33] model of solvation.

Acknowledgments

The SSRL Biotechnology Program is supported by the National Institutes of Health, National Center for Research Resources, Biomedical Technology Program, and the Department of Energy, Office of Biological and Environmental Research. This work was supported in part by grants CA 63081 (R.M.S.) and SBIR CA96262 (Kosan) from the U.S. Public Health Service.

Received: January 6, 2003
Revised: March 27, 2003
Accepted: March 27, 2003
Published: April 21, 2003

References

1. Chavany, C., Mimnaugh, E., Miller, P., Bitton, R., Nguyen, P., Trepel, J., Whitesell, L., Schnur, R., Moyer, J., and Neckers, L. (1996). p185erbB2 binds to GRP94 in vivo. Dissociation of the p185erbB2/GRP94 heterocomplex by benzoquinone ansamycins precedes depletion of p185erbB2. J. Biol. Chem. *271*, 4974–4977.
2. Minet, E., Mottet, D., Michel, G., Roland, I., Raes, M., Remacle, J., and Michiels, C. (1999). Hypoxia-induced activation of HIF-1: role of HIF-1alpha-Hsp90 interaction. FEBS Lett. *460*, 251–256.
3. Segnitz, B., and Gehring, U. (1997). The function of steroid hormone receptors is inhibited by the hsp90-specific compound geldanamycin. J. Biol. Chem. *272*, 18694–18701.
4. Stebbins, C.E., Russo, A.A., Schneider, C., Rosen, N., Hartl, F.U., and Pavletich, N.P. (1997). Crystal structure of an Hsp90-geldanamycin in complex: targeting of a protein chaperone by an antitumor agent. Cell *89*, 239–250.
5. Roe, S.M., Prodromou, C., O'Brien, R., Ladbury, J.E., Piper, P.W., and Pearl, L.H. (1999). Structural basis for inhibition of the Hsp90 molecular chaperone by the antitumor antibiotics radicicol and geldanamycin. J. Med. Chem. *42*, 260–266.
6. Supko, J.G., Hickman, R.L., Grever, M.R., and Malspeis, L. (1995). Preclinical pharmacologic evaluation of geldanamycin as an antitumor agent. Cancer Chemother. Pharmacol. *36*, 305–315.
7. Schnur, R.C., Corman, M.L., Gallaschun, R.J., Cooper, B.A., Dee, M.F., Doty, J.L., Muzzi, M.L., Moyer, J.D., DiOrio, C.I., Barbacci, E.G., et al. (1995). Inhibition of the oncogene product p185erbB-2 in vitro and in vivo by geldanamycin and dihydrogeldanamycin derivatives. J. Med. Chem. *38*, 3806–3812.
8. Schnur, R.C., Corman, M.L., Gallaschun, R.J., Cooper, B.A., Dee, M.F., Doty, J.L., Muzzi, M.L., DiOrio, C.I., Barbacci, E.G., Miller, P., et al. (1995). erbB-2 oncogene inhibition by geldanamycin derivatives: synthesis, mechanism of action, and structure-acitivity relationships. J. Med. Chem. *38*, 3813–3820.
9. Egorin, M.J., Lagattuta, T.F., Hamburger, D.R., Covey, J.M., White, K.D., Musser, S.M., and Eiseman, J.L. (2002). Pharmacokinetics, tissue distribution, and metabolism of 17-(dimethylaminoethylamino)-17-demethoxygeldanamycin (NSC 707545) in CD2F1 mice and Fischer 344 rats. Cancer Chemother. Pharmacol. *49*, 7–19.
10. Hickey, E., Brandon, S.E., Smale, G., Lloyd, D., and Weber, L.A. (1989). Sequence and regulation of a gene encoding a human 89-kilodalton heat shock protein. Mol. Cell. Biol. *9*, 2615–2626.
11. Rinehart, K.L., Jr., and Shield, L.S. (1976). Chemistry of the ansamycin antibiotics. Fortschr. Chem. Org. Naturst. *33*, 231–307.
12. Schnur, R., and Corman, M.L. (1994). Tandem [3,3]-sigmatropic rearrangements in an ansamycin-stereospecific conversion of an (S)-allylic alcohol to an (S)-allylic amine derivative. J. Org. Chem. *59*, 2581–2584.
13. Kong, Y., Shen, Y., Warth, T.E., and Ma, J. (2002). Conformational pathways in the gating of Escherichia coli mechanosensitive channel. Proc. Natl. Acad. Sci. USA *99*, 5999–6004.
14. Ma, J., and Karplus, M. (1997). Molecular switch in signal transduction: reaction paths of the conformational changes in ras p21. Proc. Natl. Acad. Sci. USA *94*, 11905–11910.
15. Ma, J., Sigler, P.B., Xu, Z., and Karplus, M. (2000). A dynamic model for the allosteric mechanism of GroEL. J. Mol. Biol. *302*, 303–313.
16. Leslie, A.G. (1999). Integration of macromolecular diffraction data. Acta Crystallogr. D Biol. Crystallogr. *55*, 1696–1702.
17. CCP4. (1994). CCP4 suite: programs for protein crystallography. Acta Crystallogr. D Biol. Crystallogr. *50*, 760–763.
18. Brunger, A.T., Adams, P.D., Clore, G.M., DeLano, W.L., Gros, P., Grosse-Kunstleve, R.W., Jiang, J.S., Kuszewski, J., Nilges, M., Pannu, N.S., et al. (1998). Crystallography & NMR system: A new software suite for macromolecular structure determination. Acta Crystallogr. D Biol. Crystallogr. *54*, 905–921.
19. Jones, T.A., Zou, J.Y., Cowan, S.W., and Kjeldgaard, M. (1993). Improved methods for building protein models in electron density maps and the location of errors in these models. Acta Crystallogr. D Biol. Crystallogr. *49*, 148–157.

20. Kraulis, P.J. (1991). MOLSCRIPT: a program to produce both detailed and schematic plots of protein structures. J. Appl. Crystallogr. *50*, 869–873.
21. Case, D.A., Pearlman, D.A., Caldwell, J.W., Cheatham, T.E., 3rd, Wang, J., Ross, W.S., Simmerling, C.L., Darden, T.A., Merz, K.M., Stanton, R.V., et al. (2002). AMBER7 (San Francisco: University of California, San Francisco).
22. Cornell, W.D., Cieplak, P., Bayly, C.I., Gould, I.R., Merz, K.M., Ferguson, D.M., Spellmeyer, D.C., Fox, T., Caldwell, J.W., and Kollman, P.A. (1995). A second generation force field for the simulation of proteins, nucleic acids, and organic molecules. J. Am. Chem. Soc. *117*, 5179–5197.
23. Ferrin, T.E., Huang, C.C., Jarvis, L.E., and Langridge, R. (1988). The MIDAS display system. J. Mol. Graph. *6*, 13–27.
24. Bayly, C.I., Cieplak, P., Cornell, W.D., and Kollman, P.A. (1993). A well-behaved electrostatic potential based method using charge restraints for deriving atomic charges-the RESP model. J. Phys. Chem. *97*, 10269–10280.
25. Tsui, V., and Case, D.A. (2000). Theory and applications of the generalized Born solvation model in macromolecular simulations. Biopolymers *56*, 275–291.
26. Tsui, V., and Case, D.A. (2000). Molecular dynamics simulations of nucleic acids with a generalized born solvation model. J. Am. Chem. Soc. *122*, 2489–2498.
27. Rychaert, J.P., Ciccotti, G., and Berendsen, H.J.C. (1977). Numerical integration of the cartesian equations of motion of a system with constraints: molecular dynamics of nalkanes. J. Comput. Phys. *23*, 327–341.
28. Schlitter, J., Engels, M., and Kruger, P. (1994). Targeted molecular dynamics: a new approach for searching pathways of conformational transitions. J. Mol. Graph. *12*, 84–89.
29. Kollman, P.A., Massova, I., Reyes, C., Kuhn, B., Huo, S., Chong, L., Lee, M., Lee, T., Duan, Y., Wang, W., et al. (2000). Calculating structures and free energies of complex molecules: combining molecular mechanics and continuum models. Acc. Chem. Res. *33*, 889–897.
30. Hawkins, G.D., Giesen, D.J., Lynch, G.C., Chambers, C.C., Rossi, I., Storer, J.W., Li, J., Zhu, T., Thompson, J.D., Winget, P., et al. AMSOL Version 6.8 (Minneapolis, MN: University of Minnesota).
31. Honig, B., and Nicholls, A. (1995). Classical electrostatics in biology and chemistry. Science *268*, 1144–1149.
32. Connolly, M.L. (1983). Analytical molecular surface calculation. J. Appl. Crystallogr. *16*, 548–558.
33. Cramer, C.J., and Truhlar, D.G. (1992). An SCF solvation model for the hydrophobic effect and absolute free energies of solvation. Science *256*, 213–217.